

# Coupling of optical characterization with particle and network synthesis for biomedical applications

## Liguo Song

State University of New York at Stony Brook  
Chemistry Department  
Stony Brook, New York 11794-3400

## Tianbo Liu

Brookhaven National Laboratory  
Department of Physics  
Upton, NY 11973-3400

## Dehai Liang

State University of New York at Stony Brook  
Chemistry Department  
Stony Brook, New York 11794-3400

## Chunhung Wu

Tamkang University  
Department of Chemistry  
Tamsui 251, Taiwan

## Vladimir S. Zaitsev

## Pierre A. Dresco

## Benjamin Chu

State University of New York at Stony Brook  
Chemistry Department  
Stony Brook, New York 11794-3400

**Abstract.** Polymeric microspheres containing a magnetic core have been used in cancer therapy for biophysical targeting of antitumor agents and in magnetic resonance imaging as contrasting agents. For the Human Genome Project, deoxyribose nucleic acid (DNA) capillary electrophoresis has become the most widely used analytical technique where a key component is the design of an effective separation medium. The synthesis and optical characterization of polymeric coated superparamagnetic nanoparticles and of (self-assembled) polymeric networks by means of a range of physical techniques, including laser light scattering and laser-induced fluorescence detection, are presented. (1) Polymeric microspheres with a superparamagnetic core. A water-in-oil microemulsion approach has been used successfully to synthesize the superparamagnetic core and the polymeric microsphere in one continuous step. The synthesis permits us to control the magnetic nanoparticle size and the thickness of the hydrogel, ranging from 80 to 320 nm. Magnetite concentration in the microspheres, calculated by vibrating-sample magnetometry, was found to be up to 3.3 wt%. The internal structure of the microspheres, as observed by atomic force microscopy, confirmed a core-shell model. (2) Development of new separation media for DNA capillary electrophoresis. Block copolymers in selective solvents can self-assemble to form supramolecular structures in solution. The nanostructures can be characterized in the dilute concentration regime by means of laser light scattering. At semidilute concentrations, the mesh size, the supramolecular structure, and the surface morphology can be investigated by means of small angle x-ray scattering and atomic force microscopy. The structural knowledge and the information on chain dynamics can then be correlated with electrophoresis using laser-induced fluorescence detection to provide a deeper understanding for the development of new separation media. © 2002 Society of Photo-Optical Instrumentation Engineers. [DOI: 10.1117/1.1482380]

**Keywords:** polymeric magnetic particles; DNA separation medium; capillary electrophoresis; laser light scattering; small angle x-ray scattering; atomic force microscopy.

Paper JBO 01009 received Jan. 29, 2001; revised manuscript received Jan. 17, 2002; accepted for publication Jan. 22, 2002.

## 1 Introduction

Over the past decade, the use of magnetite particles as magnetic resonance imaging contrast agents for magnetic resonance imaging (MRI) has been of great interest,<sup>1,2</sup> mainly because magnetite particles have nearly a 50-fold greater magnetic susceptibility than gadolinium chelates approved for use in MRI. Recently, magnetic particles have also been used in site-specific drug delivery.<sup>3</sup> However, due to the bioincompatibility of the magnetite particles, they are generally used as cores of polymeric microspheres. Different polymeric microspheres such as proteins,<sup>4–6</sup> lipids,<sup>7</sup> and synthetic<sup>8–10</sup> or natural<sup>11–13</sup> polymers have been tried, but they are generally rapidly removed from circulation. An advance in the medical application of the magnetite particles depends on new syn-

thetic methods of the polymeric microspheres with better control of the size distribution and of the surface properties.

Several techniques have been developed recently for the synthesis of various types of nanoparticles. Precipitation reactions in microemulsions offer the ability to produce ultrafine particles with controllable small sizes and uniform distributions. Polymerization in microemulsions has also been used for the preparation of polymeric microspheres to encapsulate the inorganic nanoparticles, and on one occasion the magnetic particles,<sup>14</sup> but in the micron size range.

The Human Genome Project (HGP)<sup>15</sup> is possibly the most important human scientific activity over the past decade. Recently, the completion of the rough draft of the human genome has been announced and the HGP is in an accelerated phase now to complete the project by 2003.<sup>16</sup> The completion of the HGP has considerable medical significance since most

Address all correspondence to Benjamin Chu, State University of New York at Stony Brook, Department of Chemistry, Stony Brook, NY 11794-3400. Tel: +631-632-7928; Fax: +631-632-6518; E-mail: bchu@notes.cc.sunysb.edu

disease causing genes will be identified in due course. Small alterations in deoxyribose nucleic acid (DNA) sequence of the disease causing genes can lead to many diseases such as cancer, diabetes, heart disease, myocardial infarction, atopy, atherosclerosis, cystic fibrosis, and Alzheimer's disease. DNA diagnosis for human diseases will, therefore, be realized by the analysis of the alterations that can provide valuable information for the design of DNA-based drugs for gene therapy. The need for further development of analytical methods for human disease diagnosis and DNA-based drug analysis is obvious. From this viewpoint, slab gel electrophoresis cannot meet the requirements for the analysis of huge quantities of products generated from polymerase chain reaction for the detection of human disease caused by gene defects. Capillary electrophoresis (CE), due to its high speed, easy automation, and feasibility of multiple capillary operations, is one of the main analytical techniques for this purpose.

The essential requirement for an effective separation of DNA fragments by CE is a separation medium, generally a polymer solution. A number of polymers have been exploited as DNA separation media by CE over the past decade. Some of them are methylcellulose,<sup>17</sup> hydroxypropyl-methylcellulose,<sup>18,19</sup> hydroxyethylcellulose,<sup>19-23</sup> hydroxypropylcellulose,<sup>24</sup> polyethylene oxide (PEO),<sup>25,26</sup> polyvinylpyrrolidone (PVP),<sup>27</sup> and polyacrylamide<sup>28-32</sup> as well as derivatives of polyacrylamide.<sup>33-36</sup> The DNA separation mechanism by these polymer solutions is usually described by the movement of DNA fragments through the pores formed by the random entanglement of the polymer chains. To ensure enough entanglement of the polymer chains, the polymer is generally required to have high molecular weight, and high enough polymer concentration. Therefore, the separation medium usually has high viscosity and its injection into the narrow-bore capillary (<100  $\mu\text{m}$  inner diameter) becomes a hindrance for automation.

Another requirement for the separation of DNA fragments by CE is to prevent the adsorption of DNA fragments onto the inner wall of a fused silica capillary. Chemically coated capillaries have been usually used for this purpose.<sup>37</sup> However, the coating methods increase their cost by requiring *in situ* synthesis and often give rise to problems such as capillary fouling, coating inhomogeneity, and limited lifetime. In regards to these problems, an alternative dynamic coating protocol using the molecular interaction (mainly hydrogen bond) between the Si-OH group of the capillary inner wall and the separation medium appears more promising. However, only several polymers such as PEO,<sup>26</sup> polydimethylacrylamide,<sup>33,34</sup> and PVP<sup>27</sup> can provide strong enough interactions to obtain the dynamic coating requirement.

In this paper, a synthetic procedure for the preparation of polymeric microspheres containing a magnetic core is described.<sup>38</sup> A water-in-oil microemulsion has been used as the reaction medium of both the magnetic particle and the polymeric microsphere, making the preparation easier to manipulate. The polymeric magnetic microspheres were characterized by dynamic light scattering (DLS), vibrating-sample magnetometry, (VSM) and atomic force microscopy (AFM) analysis. For DNA separation, we introduced several different kinds of polymers with dynamic coating ability, and very low viscosity at appropriate conditions for the easy introduction into the capillary. The polymer solutions have been character-

ized in the dilute concentration regime by means of laser light scattering (LLS) and in separation concentrations by means small angle x-ray scattering (SAXS), and AFM. The structural knowledge and the information on chain dynamics have then been correlated with electrophoresis to provide a deeper understanding for the development of new separation media

## 2 Experiment

### 2.1 Materials

Ferric chloride tetrahydrate, ferrous chloride tetrahydrate, tetramethylammonium hydroxide (TMAOH), toluene, methacrylic acid (MAA), 2,2'-azobisisobutyronitrile (AIBN) were purchased from Aldrich (Milwaukee, WI). Sodium bis-2-ethylhexylsulfosuccinate [aerosol OT (AOT)] was purchased from Fluka (Buchs, Switzerland). Hydroxyethyl methacrylate (HEMA) was purchased from Sigma (St. Louis, MO). *N'*-methylenebisacrylamide was purchased from Polysciences, Inc. (Warrington, PA). Before use, MAA and HEMA were distilled under 10 mm Hg at 40 and 97 °C, respectively, in the presence of copper shavings to remove the inhibitor. AIBN was recrystallized in ethanol, dried under vacuum, and stored in a refrigerator before use.

F127 was obtained as a gift from the BASF Corporation (Parsippany, NJ). B<sub>6</sub>E<sub>46</sub>B<sub>6</sub> and B<sub>10</sub>E<sub>271</sub>B<sub>10</sub> triblock copolymer samples were obtained as gifts from the Dow Chemical Co. (Freeport, TX) with E denoting oxyethylene and B denoting oxybutylene, respectively. B<sub>6</sub>E<sub>46</sub>B<sub>6</sub> and B<sub>10</sub>E<sub>271</sub>B<sub>10</sub> triblock copolymer were purified by hexane to remove the hydrophobic impurities.<sup>39</sup> For B<sub>10</sub>E<sub>271</sub>B<sub>10</sub>, because of its high melting temperature, the vacuum extraction process was done at higher temperature (about 110 °C). Triblock copolymer solutions were prepared by mixing the polymers with solvents, such as, 1X TBE buffer [89 mM Tris, 89 mM boric acid, and 2 mM ethylenediaminetetraacetic acid (EDTA) in de-ionized water] or H<sub>2</sub>O to the desired concentrations. Tris(hydroxymethyl)aminomethane (Tris), boric acid, EDTA, and ethidium bromide were purchased from Sigma. The water used in all solutions was deionized (18.2 M $\Omega$ ) with a Milli-Q water purification system (Millipore, Worcester, MA). The buffer solution was filtered by Millipore sterile membrane filters (0.45  $\mu\text{m}$  pore size) before use. The polymer solutions were then stored in the refrigerator at 4 °C for a few days before use.

The  $\phi$ X174/HaeIII digest was purchased from New England Biolabs, Inc. (Beverly, MA) and was diluted to 10  $\mu\text{g}/\text{mL}$  by using 1  $\times$  TE buffer (10 mM Tris-HCl + 1 mM EDTA) before use.

### 2.2 Synthesis of Polymeric Magnetic Particles

Both the magnetic particles and the polymeric shell were synthesized in a water-in-oil microemulsion in a continuous process. First, magnetite particles were synthesized by coprecipitation of Fe(II) and Fe(III) salts using TMAOH in the water pools of the water-in-oil microemulsion. The aqueous phase of the microemulsion was made of 0.16 g ferrous chloride tetrahydrate and 0.28 g ferric chloride tetrahydrate dissolved in 3 mL water. The oil phase of the microemulsion was made of 25 g AOT dissolved in 50 ml toluene. After deoxygenation of the aqueous solution and the AOT/toluene solution, the microemulsion was prepared by dispersing the aqueous solution into the AOT/toluene solution. 3 mL of deoxygenated 10

wt % TMAOH aqueous solution was then added to the microemulsion. The diffusion of the molecules of the base in the microemulsion was very fast and the pale yellow solution turned instantaneously intense black, proof of the precipitation of the magnetite nanoparticles. The final solution was further stirred for 20 min, being still deoxygenated.

After preparation of the magnetite particles in the microemulsion, coating of the particles with copolymers of MAA and HEMA was then followed by microemulsion polymerization. Water, monomers (MAA/HEMA=9:1 molar ratio), crosslinker, and AIBN were added to the reaction mixture in the desirable proportion under nitrogen. Several ratios of water/AOT were used. The microemulsion was then purged with nitrogen for 15 min. The polymerization of monomer was carried out at 55 °C. The reaction took place very fast. It was evidenced by a rapid change in the transparency of the microemulsion to a slightly opaque coloration. The final product remained transparent, yellow-beige in color with viscosity similar to that prior to polymerization, providing indirect support for a polymerization process, taking place exclusively inside the droplets.

The microemulsion containing the magnetite particles or the polymeric magnetic particles was very stable. No sedimentation was observed after a few months. No sedimentation was observed even with the solution placed on top of an electromagnet (ERIEZ Magnetics Model SL4, maximum magnetic field 2 kOe, magnetic field gradient at 2 cm from the poles 0.2 kOe/cm) for 48 h. The magnetite particles or the polymeric magnetic particles were recovered by precipitation in an excess of an acetone-methanol mixture (9:1 ratio), followed by several washings, centrifuged, and dried under vacuum.

### 2.3 Viscosity Determination

A Brookfield digital viscometer (model LVTDCP) was used to determine the viscosity of the polymer samples at different temperatures. The temperature was controlled by using a Lauda K-2/R circulator.

### 2.4 Laser Light Scattering

A laboratory-built laser light scattering spectrometer with the laser operating at a wavelength of 514.5 nm and an output power of about 600 mW was used to perform static light scattering (SLS) and DLS (vertically polarized incident-vertically polarized scattered light) measurements over an angular range of 15°–140°. The intensity-intensity time correlation function was measured by using a Brookhaven BI-9000 digital correlator. CONTIN analysis<sup>40</sup> was used to analyze DLS results. Detailed descriptions on SLS and DLS can be found in our earlier work.<sup>39</sup>

### 2.5 Small Angle X-Ray Scattering Experiments

SAXS experiments were performed at the X3A2 State University of New York Beam Line, National Synchrotron Light Source at Brookhaven National Laboratory, using a laser-aided prealigned pinhole collimator. The incident beam wavelength ( $\lambda$ ) was tuned at 0.154 nm. Fuji imaging plate was used as the detection system. The sample-to-detector distance was 1085 mm. The experimental data were corrected for background scattering and sample transmission.

### 2.6 Vibrating-Sample Magnetometry Analysis

The VSM (model 1660, Digital Measurement System, Inc.) was used to study the magnetic properties of magnetite particles in fields up to 16 kOe.

### 2.7 Atomic Force Microscopy Analysis

Atomic force microscopy was carried out with a nanoscope dimension microscope (Digital Instruments). Images were performed using the tapping mode with a Si<sub>2</sub>N<sub>3</sub> tip. The nanoparticle samples on silicon surface were prepared by dipping a hydrophilic silicon substrate in and then removing it from an aqueous suspension of the particle. The 21.2 w/v % F127 sample on a silicon surface was prepared by dipping a hydrophilic silicon substrate and then removing it from 1 M HCl at room temperature, followed by dipping in and then removing it from a 21.2 w/v % F127/H<sub>2</sub>O solution at 4 °C. The silicon chip was raised to room temperature before measurement. The hydrophilic silicon substrates were prepared by using a modified Shiraki treatment.

### 2.8 Capillary Electrophoresis

(CE) separation was performed using a lab-built capillary electrophoresis system. The laser-induced fluorescence detection used an argon-ion laser operating at a wavelength of 488 nm with a 5 mW output power. The fluorescence was collected by using a Zeiss epillumination fluorescence microscope and a Hamamatsu R928 photomultiplier tube.<sup>32</sup> A 13 cm 100 mm ID fused silica capillary (Polymicro Technologies, Phoenix, AZ) was flushed with 1 M HCl for 10 min. A detection window of 1.5 mm width was opened at the predetermined length from the cathodic end by stripping the polyimide coating off the capillary with a razor blade. Both cathode and anode reservoirs (1.6 mL volume) were filled with 1×TBE buffer containing 3  $\mu$ g/mL ethidium bromide. The separation medium was injected into the capillary tubing by using a 50  $\mu$ L syringe. The capillary tubing was then assembled onto the holder and a prerun at a constant electric field strength of 200 V/cm was used to introduce ethidium cation into the capillary and to stabilize the current. The DNA sample was electrokinetically injected into the capillary. The capillary temperature was controlled by thermostating the water jacket of the aluminum capillary holder with a Lauda circulator. A precision thermistor (Fenwal Electronics, Farmingham, MA) was attached to the capillary holder for temperature measurements.

## 3 Results and Discussion

### 3.1 Characterization of Polymeric Magnetic Particles

DLS was used to obtain the information on the average size and size distribution of the magnetite particles and the polymeric magnetite particles. The average hydrodynamic radius  $R_H$  of the magnetite particles was 7.3 nm with a variance of 0.24. The average hydrodynamic radius  $R_H$  for the polymeric magnetite particles was found to be equal to 80 nm with a smaller variance of 0.02. The corresponding angular dependence of the average diffusion coefficients for magnetite particles and polymeric magnetite particles is shown in Figure 1, curves a and b, respectively. It is seen from Figure 1 that the



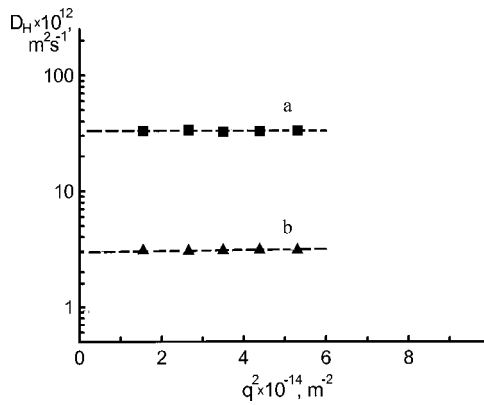


**Fig. 1** Angular dependence of diffusion coefficient of magnetic particles (a) and polymeric magnetite particles (b) (reproduced from Ref. 38 with permission).

diffusion coefficient revealed a very small angular dependence. This behavior usually suggests a small polydispersity in the size distribution. As the measured diffusion coefficient is a form of  $z$ -average diffusion coefficient, the larger particles with sizes approaching the incident light wavelength should scatter more strongly with decreasing scattering angles and result in a decrease in the average diffusion coefficient.

The magnetite particles and the polymeric magnetite particles were also analyzed by VSM. The saturation magnetization of the synthetic magnetite particles was found to be equal to 81 emu/g. This value is comparable to the theoretical value of 92 emu/g and is one of the highest values found in the literature for synthetic magnetite particles.<sup>41</sup> The saturation magnetization of the polymeric magnetite particles was found to be equal to 2.72 emu/g, representing a magnetic content of 3.3 wt % by using the reference value of the magnetite particles. Figure 2 shows a typical saturation magnetization curve of the polymeric magnetite particles with the hysteresis loop, which is characteristic of the ferrimagnetic behavior. The superparamagnetic character of the polymeric magnetite particles, which is due to the small size of the particles, can be clearly seen in the inset of Figure 2.

The polymeric magnetite particles were also examined by AFM. Figures 3(a) and 3(b) show the results obtained in the phase and the height modes, respectively. The height mode

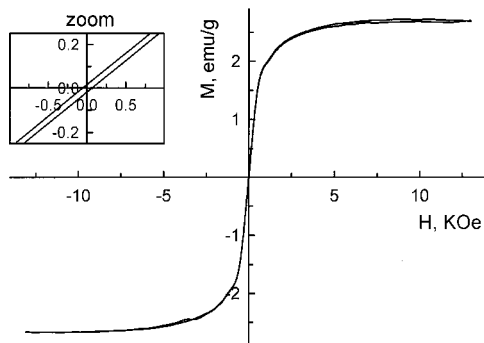


**Fig. 2** Magnetization curve for polymeric magnetic particles synthesized in one microemulsion (reproduced from Ref. 38 with permission).

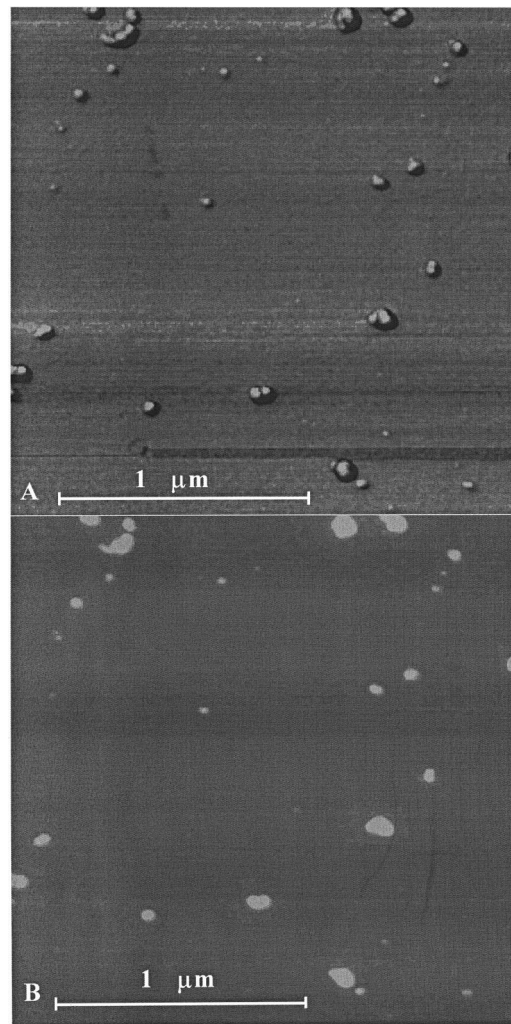


**Fig. 3** Atomic force microscopy image of polymeric magnetite particles synthesized in one microemulsion: (a) phase mode and (b) height mode (reproduced from Ref. 38 with permission).

allowed us to have the image of the global shape of the polymeric magnetite particles, but the internal image of the magnetite cores could not be seen. In the phase mode, the magnetite core was represented as a bright sphere and the polymeric shell was symbolized by a dark corona coating the core. It is noted that essentially only one core was contained in each polymeric magnetite particle.

By controlling the water/surfactant ratio of the microemulsion reaction media, the thickness of the polymeric shell could be controlled over a wide size range of 80–320 nm with similar size distributions.<sup>38</sup> In this respect, microemulsions offer the best reaction media to produce ultrafine particles due to their small sizes and uniform distributions. The technique of synthesizing a core and a shell in a single microemulsion has significantly simplified the procedure. This synthesis technique should be suitable for the synthesis of a wide variety of polymeric nanoparticles. The new synthesized magnetic hydrogel particles, made of a superparamagnetic magnetite core coated with a polymeric shell of *P*(MA/HEMA), represents a first step toward biomedical and MRI applications.

### 3.2 Investigation of F127 as New DNA Separation Medium for CE (Ref. 42)

Pluronic polyols, which are triblock copolymers consisting of a central block of poly(propylene oxide) (PPO) (or simply  $P_x$  with P denoting oxypropylene and  $x$  the number of P segments) and end blocks of PEO (or simply  $E_x$  with E denoting oxypropylene and  $x$  the number of E segments), exhibit very interesting physical properties when dissolved in water. At low temperature and low polymer concentration, the triblock copolymer is soluble in an aqueous solution because both blocks are soluble. Such a polymer solution behaves like a Newtonian fluid with relatively low viscosity even at fairly high polymer concentrations since the triblock copolymers have relatively low molecular weights. Increasing the temperature causes an increase in the hydrophobicity of the PPO block and leads to micellar formation. At an appropriate concentration and temperature, the micelles in the solution can overlap with each other, cause a sharp increase in the viscosity and yield a gel-like structure, which makes it a potential candidate as a DNA separation medium.

According to empirical rules, Pluronic polyols will not form gel-like structures if the molecular weight of the PPO block is less than about 30 PO units. Moreover, the larger the PPO block and the greater the PEO content, the greater is the gelling ability of the Pluronic polyols. We chose F127,<sup>43,44</sup> i.e.,  $E_{99}P_{69}E_{99}$ , as the test objects among the existing available commercial Pluronic polyols. Figure 4(a) shows the temperature dependence of the viscosity of 21.2 w/v % F127 solution in 1×TBE buffer. At 4 °C, the solution viscosity was about 50 cP. With increasing temperature, the solution viscosity decreased slightly from 4 to 12 °C and then increased sharply starting at about 17 °C. Measurements could not be performed at temperatures higher than 19 °C because the viscosity was so high that it exceeded the instrumentation limit. The sol-gel phase diagram of F127 solution in 1×TBE is shown in Figure 4(b).

The application of F127 as a DNA separation medium is demonstrated in Figure 5. The F127 solution in 1×TBE was filled into the capillary tubing very easily by using a 50  $\mu$ L syringe at 4 °C. F127 also has the unique ability to dynamically coat the inner wall of a fused silica capillary through hydrogen bond as PEO does. Figure 6 shows an AFM measurement of 21.2 w/v % F127/water system on a silica surface after 1 M HCl treatment.<sup>45</sup> The AFM result clearly shows that the micelles were closely packed on the surface with sizes in the range of 30–50 nm along the silica surface ( $x$ – $y$  dimensions), suggesting that F127 has the ability to coat the surface. The dynamic coating of F127 suppressed electroosmotic flow sufficiently and prevented the adsorption of DNA fragments on the capillary inner wall. The capillary tubing was only washed with 1 M HCl for 10 min to increase the affinity of F127 to the fused silica surface.

As shown in Figure 5(a), the DNA separation abilities of 15.9 w/v % F127 are poor. At this concentration, the polymer solution cannot form enough micelles for a closely packed supramolecular structure with overlapping shells.

When the concentration of F127 was increased to 21.2% and 28.0%, the solution became gel-like and its DNA separation ability was greatly improved as shown in Figures 5(b) and 5(c). In order to elucidate the F127 concentration effect

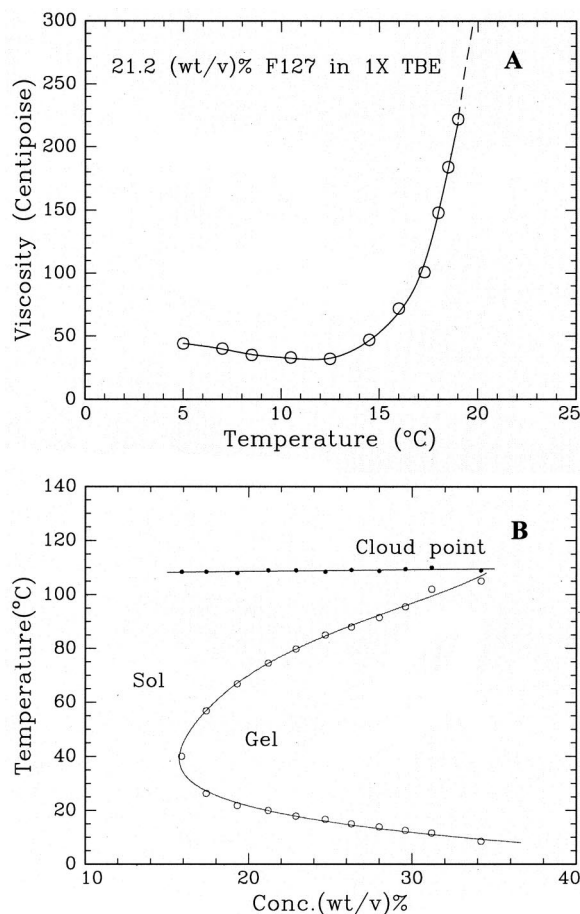


**Fig. 4** (a) Temperature dependence of the viscosity of 21.2 w/v % F127 solution in 1×TBE buffer. (b) Sol-gel phase diagram of F127 solution in 1×TBE buffer (reproduced from Ref. 44 with permission).

and temperature effect on DNA separation, the gel-like structure of F127 was investigated by SAXS. Figure 7 shows the SAXS intensity patterns of 21.2 w/v % F127 at 25 and 50 °C. The corresponding circular integration profiles in Figure 8 show seven well-resolved peaks with the ratio of relative peak position being  $1:(4/3)^{1/2}:(8/3)^{1/2}:(11/3)^{1/2}:2:(16/3)^{1/2}:(19/3)^{1/2}$ . On the basis of the Bragg diffraction peaks we were able to determine the F127 gel-like structure to have a face-centered-cubic lattice. From the similar scattering pattern at 25 and 50 °C, we could qualitatively conclude that the micelles in 21.2 w/v % F127 solution had similar sizes at both temperatures. The 28 w/v % F127 had higher micelle density, which resulted in a smaller mesh size than 21.2 w/v % F127, resulting in slower separation.

### 3.3 Investigation of Mixtures of $B_{10}E_{271}B_{10}$ and $B_6E_{46}B_6$ as New DNA Separation Medium for CE

Although DNA separation with F127 as a separation medium is quite successful, the polymer network has not been optimized. In comparison with EPE-type triblock copolymers, the self-assembly behavior of BEB-type triblock copolymers are more complicated. BEB-type triblock copolymers tend to form flower-like micelles in dilute solution. With increasing polymer concentration, theoretical and experimental results

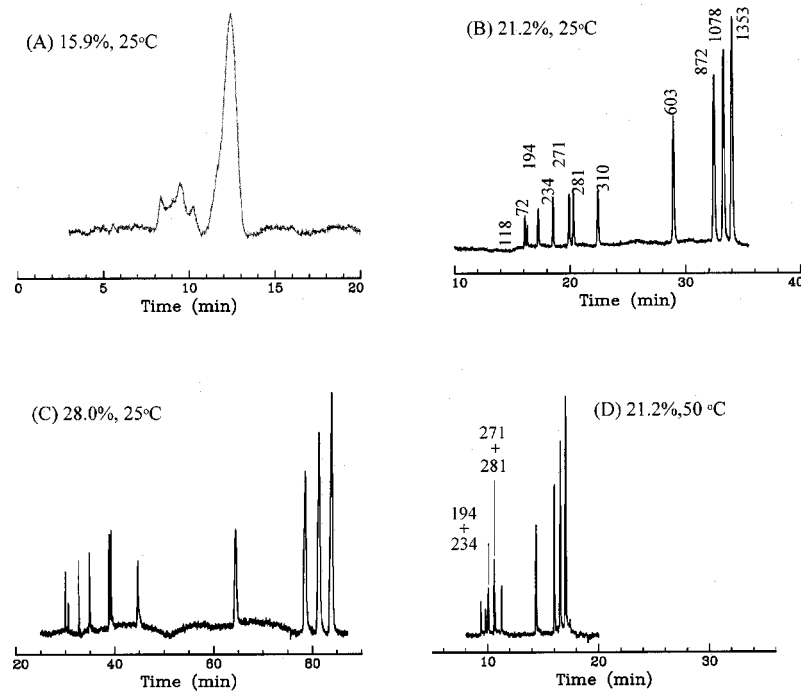


**Fig. 5** Electropherograms of  $\Phi \times 174$ /HaeIII digest obtained by using F127 as a separation medium at different concentration and temperature as indicated in the figures. The injection conditions are 300 V/cm for 5 s. The separation electric field strength is 200 V/cm. Peak identifications are shown in Figure 5(b) (reproduced from Ref. 44 with permission).

have shown that intermicellar crosslinking, instead of ordered micellar packing, should occur since water is only a good solvent for the middle block.<sup>39,46–48</sup> Consequently, the gelation concentration of BEB-type triblock copolymers is much lower than those of EBE-type triblock copolymers of comparable chain length, and also much lower than those of EPE-type triblock copolymers since B is more hydrophobic than P. Under these considerations, we tried to use  $B_{10}E_{271}B_{10}$  as new DNA separation medium, and the results are shown in Figures 9(a) and 9(b). At room temperature, 4 w/v %  $B_{10}E_{271}B_{10}$  was not gel-like, and its DNA separation ability was poor. 8 w/v %

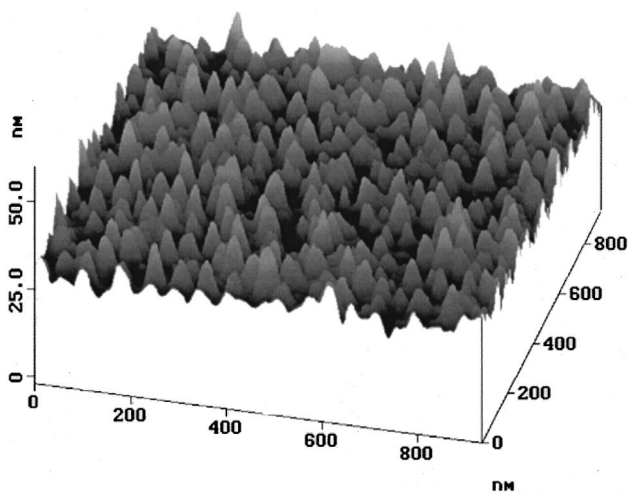


**Fig. 6** AFM measurement of 21.2 w/v % F127/water system on silica surface with Shiraki and HCl treatment (reproduced from Ref. 45 with permission).

$B_{10}E_{271}B_{10}$  was gel-like at room temperature, and consequently its DNA separation ability was improved, as shown in Figure 9(b). In comparison with the separation shown in Figures 5(b) and 5(c) using F127 as a separation medium, the separation shown in Figure 9(b) was much faster. However, the separation efficiency was lower (as evidenced by broader peaks) with correspondingly lower resolution.

In order to improve the DNA separation ability of  $B_{10}E_{271}B_{10}$ , we adopted a recent reported protocol of using mixtures of the same polymer with different molecular weight.<sup>25,26,31</sup> This protocol is based on the observation that low molecular weight polymer is good to separate small DNA fragment and high molecular weight polymer is good to separate large DNA fragments. By using mixtures of the same polymer with different molecular weight, DNA fragments over a broader size range have been efficiently separated simultaneously. A relatively small BEB-type triblock copolymers,  $B_6E_{46}B_6$ , with a concentration of 4 w/v % was mixed with 4 w/v %  $B_{10}E_{271}B_{10}$  and its DNA separation ability is demonstrated in Figure 9(c). It is observed that in comparison with 8 w/v %  $B_{10}E_{271}B_{10}$ , the mixture with the same total concentration produce faster separation with high separation efficiency and higher resolution. However, it should be noted that our BEB mixture is successful for a different and also more complex reason because the key effect deals with the self-assembling behavior of mixed micelles in a semi-open association mechanism.<sup>49</sup>

For  $B_6E_{46}B_6$ , its short B and E block lengths made it impossible for gelation to occur at room temperature even at very high polymer concentrations.<sup>39</sup> Consequently, DNA separation with this triblock copolymer was not successful. By using LLS, the nature of single and mixed triblock copoly-

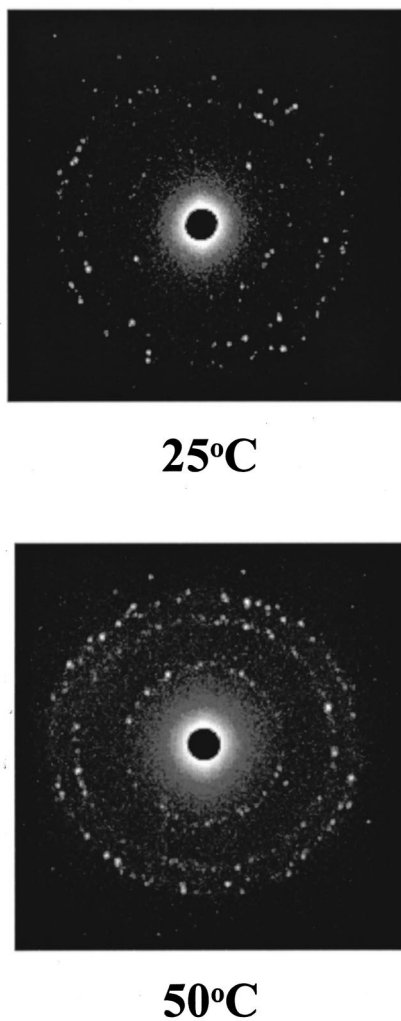


**Fig. 7** SAXS intensity patterns of 21.2 w/v % F127 in 1X TBE buffer at (a) 25 and (b) 50 °C (reproduced from Ref. 43 with permission).

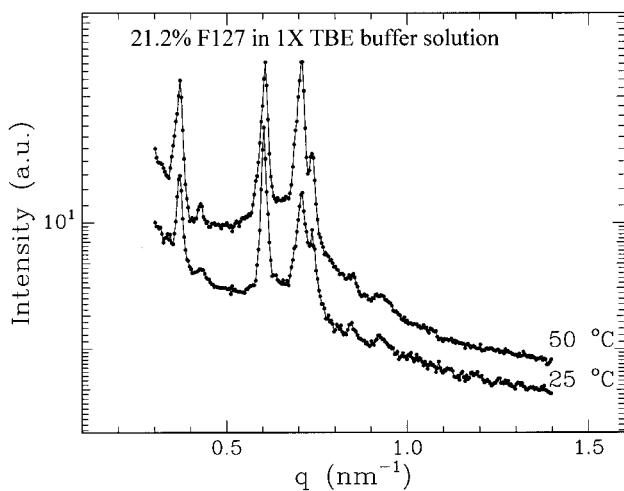


**Fig. 8** SAXS intensity profiles of 21.2 w/v % F127 in 1X TBE buffer at (a) 25 and (b) 50 °C (reproduced from Ref. 43 with permission).

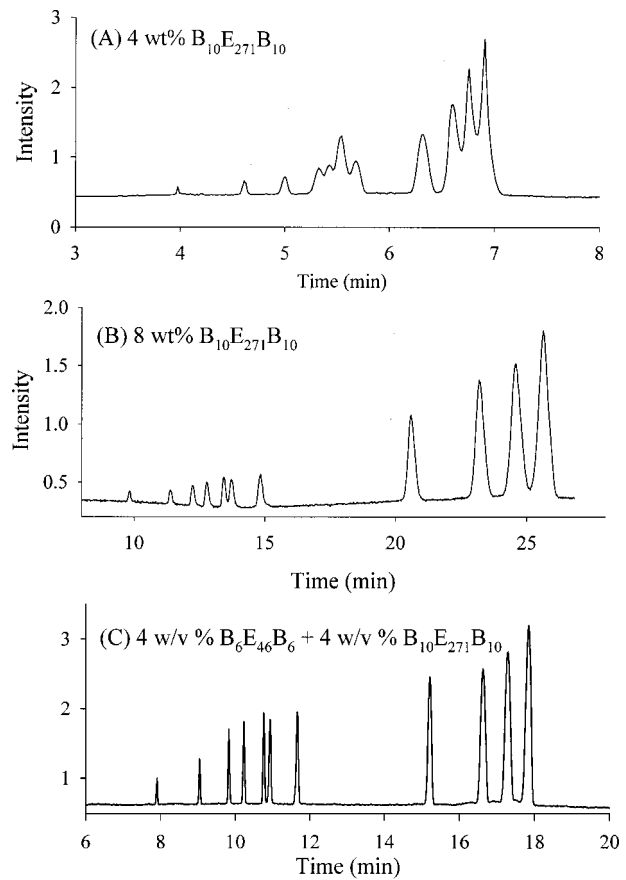


**Fig. 9** Electropherograms of  $\Phi \times 174$ /HaeIII digest obtained by using 4 w/v %  $B_{10}E_{271}B_{10}$  (a), 8 w/v %  $B_{10}E_{271}B_{10}$  (b), and 4 w/v %  $B_4E_{46}B_4$  + 4 w/v %  $B_{10}E_{271}B_{10}$  (c) as a separation medium. The injection conditions are 300 V/cm for 10 s. The separation electric field strength is 200 V/cm. Peak identifications are shown in Figure 5(b) (reproduced from Ref. 49 with permission).

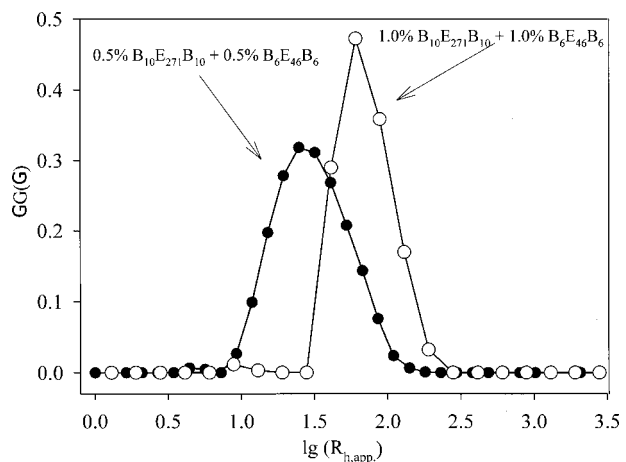


**Fig. 10** CONTIN analysis of (0.5+0.5) w/v % and (1.0 +1.0) w/v %  $B_4E_{46}B_4$  and  $B_{10}E_{271}B_{10}$  in aqueous solution. The large peaks correspond to the mixed micelles (reproduced from Ref. 49 with permission).



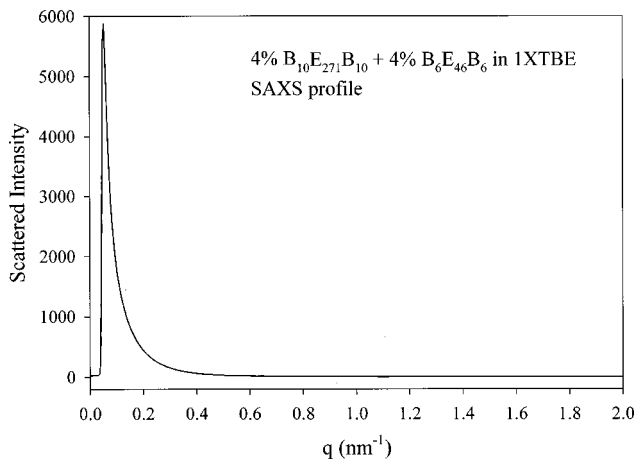


**Fig. 11** SAXS measurement on (4 + 4) w/v %  $B_4E_{46}B_4$  and  $B_{10}E_{271}B_{10}$  in  $1 \times$ TBE buffer solution. No scattering peak is observed over the entire  $q$  range ( $0.5 < q < 3.0 \text{ nm}^{-1}$ ) (reproduced from Ref. 49 with permission).

mers of  $B_6E_{46}B_6$  and  $B_{10}E_{271}B_{10}$  in dilute solutions has been studied. At room temperature, the associate number ( $N_w$ ) of single  $B_6E_{46}B_6$  and  $B_{10}E_{271}B_{10}$  micelles were estimated to be 7 and 24, respectively.<sup>39,47</sup> For the mixed copolymer solution, the more hydrophobic  $B_{10}E_{271}B_{10}$  first self-associated into micelles by themselves, then the less hydrophobic  $B_4E_{46}B_4$  gradually joined into the micelles to form mixed micelles at concentrations lower than its original critical micelle concentration.<sup>48</sup> By assuming that the weight fractions of the two kinds of copolymers in the micelles were the same, the associate number of 1:1 (in weight) mixed micelles was estimated to be 16. Therefore, in comparison with 8 w/v %  $B_{10}E_{271}B_{10}$ , 4 w/v %  $B_6E_{46}B_6$  + 4 w/v %  $B_{10}E_{271}B_{10}$  had more micelles inside the solution, which lead to a change in the number of cross-linking units.

Figure 10 shows the CONTIN analysis of (0.5 w/v % + 0.5 w/v %) and (1 w/v % + 1 w/v %)  $B_6E_{46}B_6/B_{10}E_{271}B_{10}$  solutions at 25 °C. Only one dominant peak was detected, indicating that the two triblock copolymers only formed

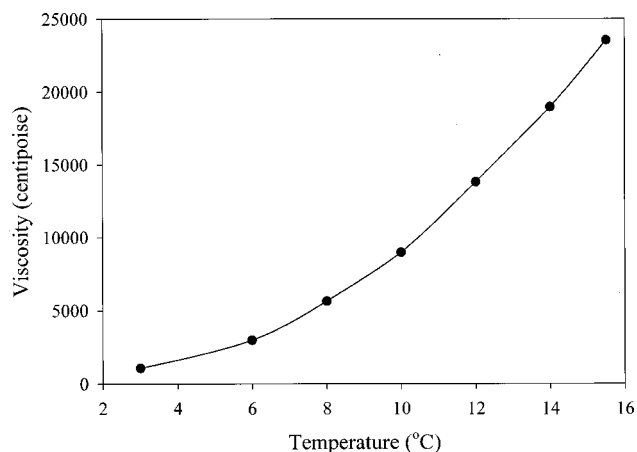


**Fig. 12** Temperature dependence of viscosity of (4 + 4) w/v %  $B_4E_{46}B_4$  and  $B_{10}E_{271}B_{10}$  in  $1 \times$ TBE buffer solution (reproduced from Ref. 49 with permission).

mixed micelles. The  $R_{h,app}$  of the latter solution was much higher than the former one, indicating very strong intermicellar attractions. Figure 11 shows SAXS measurements on 4 w/v %  $B_6E_{46}B_6$  + 4 w/v %  $B_{10}E_{271}B_{10}$  in  $1 \times$ TBE buffer. There was no obvious scattering peak in the entire  $q$  range of  $0.5\text{--}3 \text{ nm}^{-1}$ , suggesting no ordered structure in the solution. All these results were consistent with the theoretical prediction made by Tanaka et al.<sup>46</sup> Figure 12 shows the viscosity of 4 w/v %  $B_4E_{46}B_4$  + 4 w/v %  $B_{10}E_{271}B_{10}$  in  $1 \times$ TBE buffer. The sol-gel transition within the proper temperature range made it very easy to be injected into the capillary column. Besides, both  $B_4E_{46}B_4$  and  $B_{10}E_{271}B_{10}$  have dynamic coating ability to the silica surface as F127 does.

## Acknowledgments

B.C. gratefully acknowledges support of this work by the National Human Genome Research Institute (NHGRI 2R01HG0138607), the Department of Energy (DEFG 0286ER45237.016), and the National Science Foundation (DMR9984102). This work was partially done at the Physics Department, Brookhaven National Laboratory, supported by the U.S. Department of Energy, Division of Materials Science, under Contract No. DE-AC02-98CH10886.

## References

1. R. Weissleder, A. Bogdanov, and M. Papisov, "Drug targeting in magnetic resonance imaging," *Magn. Reson. Q.* **8**, 55–63 (1992).
2. R. W. Briggs, W. J. Wu, C. R. Mladinich, C. Stoupis, J. Gauger, T. Liebig, P. R. Ros, J. R. Ballinger, and P. Kubilis, "In vivo animal tests of an artifact-free contrast agent for gastrointestinal MRI," *Magn. Reson. Imaging* **15**, 559–566 (1997).
3. P. K. Gupta and C. T. Hung, "Magnetically controlled targeted micro-carrier systems," *Life Sci.* **44**, 175–186 (1989).
4. D. J. Widder, W. L. Greif, K. J. Widder, R. R. Edelman, and T. Brady, "Magnetite albumin microspheres—a new MR contrast material," *Am. J. Roentgenol.* **148**, 399–404 (1987).
5. P. F. Renshaw, C. S. Owen, A. C. McLaughlin, T. G. Frey, and J. S. Leigh, Jr., "Ferromagnetic contrast agents—a new approach," *Magn. Reson. Med.* **3**, 217–225 (1986).
6. D. P. E. Dickson, S. A. Walton, S. Mann, and K. Wong, "Properties of magnetoferritin: A novel biomagnetic nanoparticle," *Nanostruct. Mater.* **9**, 595–598 (1997).
7. J. W. M. Bulte, L. D. Ma, R. L. Magin, R. L. Kamman, C. E. Hulstaert, K. G. Go, T. H. The, and L. de Leij, "Selective MR imaging of labeled human peripheral-blood mononuclear-cells by liposome mediated incorporation of dextran-magnetite particles," *Magn. Reson. Med.* **29**, 32–37 (1993).
8. W. F. Patton, J. Kim, and B. S. Jacobson, "Rapid, high-yield purification of cell-surface membrane using colloidal magnetite coated with polyvinylamine-sedimentation versus magnetic isolation," *Biochim. Biophys. Acta* **816**, 83–92 (1985).
9. J. Lee, T. Isobe, I. Tsobe, and M. Senna, "Magnetic properties of ultrafine magnetite particles and their slurries prepared via *in-situ* precipitation," *Colloids Surf. A* **109**, 121–127 (1996).
10. G. D. Mendenhall, Y. Geng, and J. Hwang, "Optimization of long-term stability of magnetic fluids from magnetite and synthetic polyelectrolytes," *J. Colloid Interface Sci.* **184**, 519–526 (1996).
11. L. Josephson, E. V. Groman, W. Menz, J. M. Luis, and H. Bengel, "A functionalized superparamagnetic iron-oxide colloid as a receptor directed mr contrast agent," *Magn. Reson. Imaging* **8**, 637–646 (1990).
12. R. S. Molday and D. Mackenzie, "Immunospecific ferromagnetic iron-dextran reagents for the labeling and magnetic separation of cells," *J. Immunol. Methods* **52**, 353–367 (1982).
13. C. E. Sjogren, C. Johansson, A. Naevestad, P. C. Sontum, K. Briley-saebø, and A. K. Fahlvik, "Crystal size and properties of superparamagnetic iron oxide (SPIO) particles," *Magn. Reson. Imaging* **15**, 55–67 (1997).
14. D. Poulliquen, R. Perdrisot, A. Ermiyas, P. Jallet, and J. Le Jeune,



- “Superparamagnetic iron-oxide nanoparticles as a liver MRI contrast agent—contribution of microencapsulation to improved biodistribution,” *J. Magn. Reson. Imaging* **7**, 619–627 (1989).
15. J. D. Watson, “The human genome project—past, present, and future,” *Science* **248**, 44–49 (1990).
  16. E. Pennisi and L. Roberts, “Human genome project—Chromosome 21 done, phase two begun,” *Science* **288**, 939 (2000).
  17. W. A. MacCrehan, H. T. Rasmussen, and D. M. Northrup, “Size-selective capillary electrophoresis (ssce) separation of dna fragments,” *J. Liquid Chromatogr.* **15**, 1063–1080 (1992).
  18. K. C. Chan, C.-W. Whang, and E. S. Yeung, “Separation of DNA restriction fragments using capillary electrophoresis,” *J. Liquid Chromatogr.* **16**, 1941–1962 (1993).
  19. C. Gelfi, M. Perego, F. Libbra, and P. G. Righetti, “Comparison of behavior of N-substituted acrylamides and celluloses on double-stranded DNA separations by capillary electrophoresis at 25 degrees and 60 degrees C,” *Electrophoresis* **17**, 1342–1347 (1996).
  20. P. D. Grossman and D. S. Soane, “Capillary electrophoresis of DNA in entangled polymer-solutions,” *J. Chromatogr.* **559**, 257–266 (1991).
  21. B. R. McCord, J. M. Jung, and J. Hoeran, “High resolution capillary electrophoresis of forensic DNA using a nongel sieving buffer,” *J. Liquid Chromatogr.* **16**, 1963–1981 (1993).
  22. A. E. Barron, D. S. Soane, and H. W. Blanch, “Capillary electrophoresis of dna in uncross-linked polymer-solutions,” *J. Chromatogr., A* **652**, 3–16 (1993).
  23. J. Bashkin, M. Marsh, D. Barker, and R. Johnston, “DNA sequencing by capillary electrophoresis with a hydroxyethylcellulose sieving buffer,” *Appl. Theor. Electrophoresis* **6**, 23–28 (1996).
  24. L. Mitnik, L. Salome, J. L. Viory, and C. Heller, “Systematic study of field and concentration effects in capillary electrophoresis of DNA in polymer-solutions,” *J. Chromatogr., A* **710**, 309–321 (1995).
  25. H. T. Chang and E. S. Yeung, “Poly(ethyleneoxide) for high-resolution and high-speed separation of DNA by capillary electrophoresis,” *J. Chromatogr., B* **669**, 113–123 (1995).
  26. Y. Kim and E. S. Yeung, “Separation of DNA sequencing fragments up to 1000 bases by using poly(ethylene oxide)-filled capillary electrophoresis,” *J. Chromatogr., A* **781**, 315–325 (1997).
  27. Q. Gao and E. S. Yeung, “A matrix for DNA separation: Genotyping and sequencing using poly(vinylpyrrolidone) solution in uncoated capillaries,” *Anal. Chem.* **70**, 1382–1388 (1998).
  28. M. Chiari, M. Nesi, and P. G. Righetti, “Movement of DNA fragments during capillary zone electrophoresis in liquid polyacrylamide,” *J. Chromatogr., A* **652**, 31–39 (1993).
  29. Y. F. Pariat, J. Berka, D. N. Heiger, T. Schmitte, M. Vilenchik, A. S. Cohen, F. Foret, and B. L. Karger, “Separation of DNA fragments by capillary electrophoresis using replaceable linear polyacrylamide matrices,” *J. Chromatogr., A* **652**, 57–66 (1993).
  30. J. Z. Zhang, Y. Fang, J. Y. Hou, H. J. Ren, R. Jiang, P. Roos, and N. J. Dovichi, “Use of non-cross-linked polyacrylamide for 4-color DNA-sequencing by capillary electrophoresis separation of fragments up to 640 bases in length in 2 hours,” *Anal. Chem.* **67**, 4589–4593 (1995).
  31. H. Zhou, A. W. Miller, Z. Sosic, B. Buchholz, A. E. Barron, L. Kotler, and B. L. Karger, “DNA sequencing up to 1300 bases in two hours by capillary electrophoresis with mixed replaceable linear polyacrylamide solution,” *Anal. Chem.* **72**, 1045–1052 (2000).
  32. C. Wu, M. A. Quesada, D. K. Schneider, R. Farinato, F. W. Studier, and B. Chu, “Polyacrylamide Solutions for DNA Sequencing by Capillary Electrophoresis: Mesh Sizes, Separation and Dispersion,” *Electrophoresis* **17**, 1103–1109 (1996).
  33. R. S. Madabhushi, “Separation of 4-color DNA sequencing extension products in noncovalently coated capillaries using low viscosity polymer solutions,” *Electrophoresis* **19**, 224–230 (1998).
  34. C. Heller, “Finding a universal low viscosity polymer for DNA separation (II),” *Electrophoresis* **19**, 3114–3127 (1998); “Separation of double-stranded and single-stranded DNA in polymer solutions: II. Separation, peak width and resolution,” *ibid.* **20**, 1978–1986 (1999); “Separation of double-stranded and single-stranded DNA in polymer solutions: I. Mobility and separation mechanism,” *ibid.* **20**, 1962–1977 (1999).
  35. M. Chiari, F. Damin, A. Melis, and R. Consonni, “Separation of oligonucleotides and DNA fragments by capillary electrophoresis in dynamically and permanently coated capillaries, using a copolymer of acrylamide and beta-D-glucopyranoside as a new low viscosity matrix with high sieving capacity,” *Electrophoresis* **19**, 3154–3159 (1998).
  36. D. Liang, L. Song, S. Zhou, V. S. Zaitsev, and B. Chu, “Poly(N-isopropylacrylamide)-g-poly(ethyleneoxide) for high resolution and high speed separation of DNA by capillary electrophoresis,” *Electrophoresis* **20**, 2856–2863 (1999).
  37. S. Hjerten, “High-performance electrophoresis—elimination of electroendosmosis and solute adsorption,” *J. Chromatogr.* **347**, 191–198 (1985).
  38. P. A. Dresco, V. S. Zaitsev, R. J. Gambino, and B. Chu, “Preparation and properties of magnetite and polymer magnetite nanoparticles,” *Langmuir* **15**, 1945–1951 (1999).
  39. T. Liu, Z. Zhou, C. Wu, B. Chu, D. Schneider, and V. M. Nace, “Self-assembly of poly(oxybutylene)-poly(oxyethylene)-poly(oxybutylene) (B6E46B6) triblock copolymer in aqueous solution,” *J. Phys. Chem. B* **101**, 8808–8815 (1997).
  40. S. W. Provencher, “Fourier method for analysis of exponential decay curves,” *Biophys. J.* **16**, 27–41 (1976); “Eigenfunction expansion method for analysis of exponential decay curves,” *J. Chem. Phys.* **64**, 2773–2777 (1976).
  41. C. H. Lin, P. C. Kuo, J. L. Pan, and D. R. Huang, “Effects of Zn ion on magnetic properties of Fe<sub>3</sub>O<sub>4</sub> magnetic colloids,” *J. Appl. Phys.* **79**, 6035 (1996).
  42. C. Wu, T. Liu, and B. Chu, “A new separation medium for DNA capillary electrophoresis: self-assembly behavior of Pluronic polyol E99P69E99 in 1X TBE buffer,” *J. Non-Cryst. Solids* **235**, 605–611 (1998).
  43. C. Wu, T. Liu, B. Chu, D. K. Schneider, and V. Graziano, “Characterization of the PEO-PPO-PEO triblock copolymer and its application as a separation medium in capillary electrophoresis,” *Macromolecules* **30**, 4574–4583 (1997).
  44. C. Wu, T. Liu, and B. Chu, “Viscosity-adjustable block copolymer for DNA separation by capillary electrophoresis,” *Electrophoresis* **19**, 231–241 (1998).
  45. C. Wu, T. Liu, H. White, and B. Chu, “Atomic force microscopy study of E99P69E99 triblock copolymer chains on silicon surface,” *Langmuir* **16**, 656–661 (2000).
  46. F. Tanaka and M. Ishida, “Elastically effective chains in transient gels with multiple junctions,” *Macromolecules* **29**, 7571–7580 (1996).
  47. T. Liu, Z. Zhou, C. Wu, V. M. Nace, and B. Chu, “Cloud-point temperatures of BnEmBn and PnEmPn type triblock copolymers in aqueous solution,” *J. Phys. Chem. B* **101**, 8074–8078 (1997).
  48. T. Liu, V. M. Nace, and B. Chu, “Self-assembly of mixed amphiphilic triblock copolymers in aqueous solution,” *Langmuir* **15**, 3109–3117 (1999).
  49. T. Liu, D. Liang, L. Song, V. M. Nace, and B. Chu, “Spatial open-network formed by mixed triblock copolymers as a new medium for double-stranded DNA separation by capillary electrophoresis,” *Electrophoresis* **22**, 449–458 (2001).